Research Square

Preprints are preliminary reports that have not undergone peer review.
They should not be considered conclusive, used to inform clinical practice,
or referenced by the media as validated information.

DCADNT: Dynamic Topology Adaptive Data Collection Scheme Based on AUV for Mobile Underwater Wireless Sensor Networking

Xiaoyun Guang
Hebei University
Chunfeng Liu
cfliu@tju.edu.cn
Tianjin University
Zijuan Liu
Beijing College of Politics and Law
Jiaqi Shen
Hebei University
Wenlong He
Hebei University
Yanni Ma
Hebei University
Zhao Zhao
Tianjin University of Technology

Research Article

Keywords: Underwater wireless sensor network, AUV, data collection, dynamic topology, propagation delay

Posted Date: November 6th, 2026

DOI: https://doi.org/10.21203/rs.3.rs-11114690/v1

License: This work is licensed under a Creative Commons Attribution 4.0 International License.
Read Full License

Additional Declarations: No competing interests reported.

DCADNT: Dynamic Topology Adaptive Data Collection Scheme Based on AUV for Mobile Underwater Wireless Sensor Networking

Guang Xiaoyun[1,2*], Liu Chunfeng[3*†], Liu Zijuan[4], Shen Jiaqi[1,2], He Wenlong[1,2], Ma Yanni[1,2], Zhao Zhao[5]

[1*]School of Cyber Security and Computer, Hebei University, Baoding, 071002, China.
[2]Key Lab on High Trusted Information System in Hebei Province, Baoding, 071002, China.
[3]College of Intelligence and Computing, Tianjin University, Tianjin, China.
[4]Information Media Institute, Beijing College of Politics and Law, Beijing, China.
[5]School of Computer Science and Engineering, Tianjin University of Technology, Tianjin, China.

*Corresponding author(s). E-mail(s): guangxiaoyun@hbu.edu.cn; cfliu@tju.edu.cn;
†These authors contributed equally to this work.

Abstract

Underwater wireless sensor network (UWSN) has become one of the pivotal technologies in the advancement of smart oceans monitoring systems, with autonomous underwater vehicles (AUVs) offering a highly promising solution for mobile sensor data collection. In dynamic UWSN, the mobility of nodes leads to continuous network topology variations and unstable cluster structures, accompanied by dynamic cluster-head (CH) updates and intermittent acoustic communication links, which increase the difficulty and latency of AUV-based data collection. To overcome these above difficulties, this paper proposes a data collection algorithm orientated for dynamic network topology (DCADNT), consisting of three core phases: dynamic clustering with multi-criteria CH selection, propagation delay-aware adaptive dynamic transmission, and mobility prediction-based reliable AUV data collection. Different from conventional mobile

UWSN methods, DCADNT innovatively breaks the continuous communication assumption, integrates time-varying topology dynamics, acoustic propagation delay characteristics, and link reliability constraints into a unified optimization framework. By calculating the packet delivery probability based on propagation delay, the reliability of data transmission can be effectively guaranteed. Extensive simulation results demonstrate that the proposed DCADNT algorithm effectively reduces collection latency and improves packet collection reliability in dynamic underwater networks.

Keywords: Underwater wireless sensor network, AUV, data collection, dynamic topology, propagation delay

1 Introduction

Underwater wireless sensor network (UWSN) has been extensively applied in various intelligent application[1]. Equipped with mobility, storage, computation, and sensing capabilities, autonomous underwater vehicles (AUVs) serve as mobile edge nodes to support underwater data collection and transmission.

As the marine extension of terrestrial WSN, UWSN systems enable environmental monitoring, water quality assessment, and underwater resource exploration [2, 3]. A typical UWSN framework comprises surface base stations, AUVs, and underwater nodes that transmit sensed data to base stations via acoustic channels, supporting long-term marine monitoring and decision-making [4–6]. Thus, efficient, reliable, and low-latency data collection schemes are critical for stable UWSN operation. Different from static underwater networks, practical UWSN features dynamic node mobility caused by water currents. Physical oceanography studies verify that flow velocity varies with depth, remains stable at a fixed horizontal layer [7–10], and generally decreases with increasing depth[11, 12]. Although node mobility facilitates large-scale marine monitoring with limited sensor deployment, node movement creates critical obstacles for stable data collection. Different from low-mobility terrestrial WSN underwater acoustic communication suffers from low propagation speed, time-varying path loss, and severe noise interference, making mobile UWSN data collection more challenging.

Dynamic node mobility brings three key challenges for UWSN data collection. First, underwater sensors suffer from severe energy constraints, with impractical battery replacement underwater, limiting network coverage and lifetime [13, 14]. Second, acoustic communication exhibits a low propagation speed of 1.5×10^3 m/s, far lower than terrestrial radio communication (3×10^8 m/s), resulting in substantial propagation latency [15]. Third, random node drift causes frequent link interruptions, packet loss, and dynamic topology reconfiguration, which may lead to network partition and isolated sub-networks.

Notably, existing mobile UWSN algorithms do consider node mobility design, but they universally retain the ideal assumption of continuous valid communication during node movement. Most schemes can adapt to low-speed node position drift but fail to handle mobility-induced intermittent links, network segmentation, and isolated

node data loss, which severely degrades the performance of conventional data collection strategies in dynamic marine scenarios. Therefore, dynamic topology adaptive data collection algorithms with joint latency, reliability, and energy optimization are urgently required.

Existing data collection methods are categorized into multi-hop routing, AUV-aided collection, and hybrid approaches. Multi-hop routing suffers from unbalanced energy consumption, and dynamic topology changes further degrade its performance [16]. AUV-aided collection balances energy distribution via mobile cruising but introduces high collection latency. Additionally, sensor drift before AUV arrival also causes collection failure and low data reliability[17][18]. Hybrid schemes integrate multi-hop forwarding and AUV collection, where ordinary nodes relay data to CHs for AUV aggregation[19]. However, CH nodes bear heavy forwarding loads and consume excessive energy. Moreover, continuous node mobility destabilizes cluster structures, triggers frequent topology updates and CH reselection, further complicating AUV scheduling and reliable data collection.

Most existing mobile oriented UWSN algorithms focus on adaptive routing or dynamic clustering independently, without jointly coupling time-varying topology dynamics, acoustic propagation delay characteristics, and link reliability constraints. For this limitations, this paper proposes an energy-efficient, low-latency, and high-reliability data collection scheme for mobile UWSN.

This paper proposes a data collection algorithm orientated for dynamic network topology (DCADNT) that integrates multi-hop routing and AUV-aided collection. Targeting mobility-induced challenges including unstable clustering, time-varying topology, intermittent communication, uncertain node positions, and high collection delay, DCADNT optimizes collection latency, energy balance, and data efficiency to prolong network lifetime. The major contributions are summarized as follows:

- A multi-layer current model is adopted to simulate underwater node drift. A dynamic clustering and adaptive CH selection strategies are designed to adapt to time-varying network topologies.
- Cluster members transmit data to CHs through the variable routing of dynamic topology during the movement. Considering mobility-induced route variations and communication interruptions, a propagation delay-based packet delivery probability is calculated to eliminate link failure and isolated node data loss under dynamic topology partition and guarantee transmission reliability.
- A novel DCADNT algorithm is proposed to reduce collection delay, balance energy consumption, and improve data collection efficiency in dynamic UWSN.

The remainder of this paper is organized as follows. Section II reviews related works on underwater data collection. Section III presents the mobile UWSN system model. Section IV details the proposed DCADNT algorithm. The performance evaluation is presented in Section V. Finally, the main works are summarized, and prospects are discussed.

2 Related Work

Sensor nodes in mobile UWSN are classified into cable-anchored nodes and cable-free nodes. Anchored nodes experience minor position offsets under current disturbance despite cable constraints[20, 21] , while free nodes undergo wide-range irregular migration driven by marine currents, submarines, or marine organisms[22, 23]. Such widespread node position deviation fundamentally undermines the feasibility of traditional fixed-position data collection strategies.

Current data collection techniques are categorized into multi-hop routing, AUV-aided collection, and hybrid schemes. Traditional static multi-hop routing fails to adapt to dynamic environments. For anchored node offset movement, TCASI and RDA algorithms achieve adaptive multi-hop forwarding to improve coverage and energy efficiency [20, 21], yet they only apply to dense networks and ignore mobility-induced network segmentation, leading to data loss of isolated nodes. For irregular free node movement, OFAIM and MDA-SL algorithms adopt dynamic path selection for mobile data collection [24, 25], yet they assume stable continuous communication and neglect packet loss caused by dynamic link fluctuations. MLCEE layered clustering protocol based on Ekman drift reduces latency and energy consumption but suffers from serious energy imbalance among upper-layer nodes [26].

AUV-aided collection effectively mitigates the energy imbalance and topology sensitivity problems of pure multi-hop routing. Jiang et al. [27] utilized improved SAC (Soft Actor Critic) and DDPG algorithms to learn obstacle avoidance strategies through real-time interactive trial and error with the environment, greatly improving the survival rate and task completion rate of AUVs in complex unknown ocean current environments. The PHRL scheme enables obstacle avoidance via real-time direction adjustment but cannot generate optimal shortest trajectories [28]. DDCA algorithm predicts node drift positions and optimizes dynamic AUV paths, achieving higher collection efficiency in UWSN[18].

Hybrid schemes combine multi-hop forwarding and AUV-aided collection to jointly optimize energy consumption and latency, where nodes forward data to CHs for AUV aggregation. ACRL integrates fuzzy C means (FCM) and firefly algorithm (FA) to achieve clustering and cluster head optimization, and uses Q-learning to complete AUV trajectory planning [29]. The multi-AUV HAMA scheme adopts spiral cruising trajectories and selects near-path nodes as CHs to simplify forwarding, yet overloaded CHs exhaust energy prematurely and shorten network lifetime[30]. SGAPP integrates dynamic clustering and genetic path planning but ignores transmission failures caused by isolated nodes and link interruptions [31]. The layered SDCS scheme adapts to current stratification to reduce network overhead [9], yet it is only applicable to specific network models and fails to address frequent link breakage of drifting edge nodes.

Overall, existing algorithms rely on the ideal assumption of persistent inter-node communication after node movement, ignoring mobility-induced network partitioning and isolated sub-networks, which cause transmission failures and degrade collection integrity. To tackle this limitation, this paper proposes a novel data collection algorithm orientated for dynamic network topology adaptive to complex and time-varying node mobility.

3 System Model

3.1 Network model

This study investigates a problem within an underwater space described by a 3D coordinate system, as illustrated in Fig.1. The system is composed of a base station, AUV, and numerous underwater sensor nodes. A standardized coordinate system is adopted: 0m denotes the water surface, and Hm denotes the seabed. The base station is fixed on the water surface for unified simulation settings.

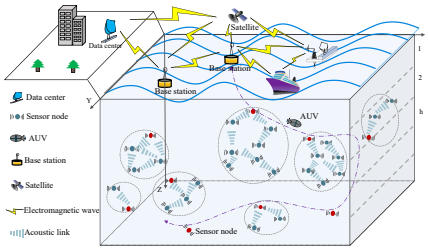


Fig. 1: Network architecture

1) **Underwater sensor nodes:** A set of sensor nodes $V = \{v_1, v_2, \ldots, v_n\}$ is randomly deployed in the 3D monitoring area. Each node v_i has a fixed communication radius R_c and residual energy $E_{res}(i) \in [0, E_0]$, where E_0 is initial energy. The coordinate of v_i at time t is $(x_i(t), y_i(t), z_i(t))$. $N_i(v_i \notin N_i)$ denotes the neighbor set of v_i, and $F_i^{cw}(F_i^{cw} \subseteq N_i)$ denotes the candidate forwarding node set with reliable packet transmission capability.

2) **Communication links:** For $\forall v_i, v_j \in V$, a valid communication link exists at time t if their Euclidean distance $d(v_i, v_j, t) \leq R_c$.

3.2 Definitions and Assumptions

Definition 1: If $d(v_i, v_j, t) \leq R_c$, node v_j is a neighbor of v_i at time t. If v_j apt to continue to successfully forward packets, v_j is the candidate forwarding node of v_i.

Definition 2: Network lifetime is defined as the number of complete data acquisition rounds executed before the first sensor node exhausts its residual energy.

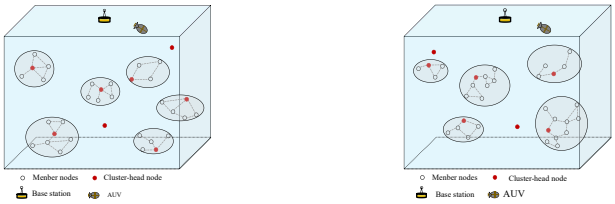
Definition 3: Data collection delay refers to the total time consumed by AUV to complete CH data collection and return to the surface base station.

Assumption 1: The AUV carries sufficient power supply and supports high-precision real-time positioning; its constant moving speed is denoted as v_{auv}.

Assumption 2: Underwater sensors only generate passive horizontal drift without self-propulsion equipment, vertical displacement is negligible.

3.2.1 Node mobility model

The H monitoring depth is equally divided into $\mathfrak{h}$ horizontal layers with depth-dependent current velocity u^h and deflection angle α^h, conforming to oceanographic



(a) (b)

Fig. 2: The dynamic changes in network topology. (a) Topology at time t. (b) Topology at time $t + \Delta t$.

characteristics that flow intensity weakens with increasing depth. The quantitative current parameters are:

$$u^h = u_{max} \cdot (1 - h/(H/\mathfrak{h})) \tag{1}$$

$$\alpha^h = \alpha_0 \cdot h/(H/\mathfrak{h}) \tag{2}$$

where $h \in \{1, 2, \ldots, H/\mathfrak{h}\}$ is the layer index, $u_{max} \in \{0.5, 1.0, 2.0\}$m/s corresponds to quasi-static, normal, and fast flow scenarios, and $\alpha_0 = \pi/6$ is the maximum deflection angle. The node dynamic position model is formulated as:

$$\begin{cases} x_i(t) = x_i(0) + u^h \cdot \cos\alpha^h \cdot t - \frac{u^h \cdot \cos\alpha^h}{\xi}[1 - e^{-\xi \cdot t}] \\ y_i(t) = y_i(0) + u^h \cdot \sin\alpha^h \cdot t - \frac{u^h \cdot \sin\alpha^h}{\xi}[1 - e^{-\xi \cdot t}] \\ z_i(t) = z_i(0), \end{cases} \tag{3}$$

where $(x_i(0), y_i(0), z_i(0))$ represents the initial position coordinate, and ξ is the inertial parameter of system, which can be calculated by (4)

$$\xi = \frac{c_0 \cdot \sigma \cdot A_R}{\rho \cdot \mathbb{V}}, \tag{4}$$

where A_R represents the node horizontal cross-sections area, ρ is node density, $\mathbb{V}$ is node volume, $c_0 = 7.2\text{Ns/m}^3$, and σ is a shape factor[12]. Similar to the research on dynamic water in [32][33], this paper mainly considers the horizontal motion of water flow and ignores the vertical motion. Thus, $z_i(t) = z_i(0)$. A passive boundary rebound mechanism is adopted, where nodes reverse drift direction automatically via environmental force when reaching the monitoring boundary, without active propulsion.

Node mobility triggers persistent network topology updates, as shown in Fig.2. Fig. 2a depicts the network topology and CH selection at time t, Fig. 2b presents the reconfigured topology and updated CHs at $t + \Delta t$ after node drift.

3.3 Energy consumption model

Node energy consumption mainly includes data transmission and reception overheads. The transmission energy consumption is

$$E_{tran}(i,j) = p_t \cdot \frac{b_{tran}(i)}{u_t} + b_{tran}(i) \cdot E_{elec}, \tag{5}$$

where E_{elec} represents the energy consumption coefficient of the transmission circuit, p_t is transmission power, $b_{tran}(i)$ is total transmitted packet size, and u_t is the transmission rate of the acoustic channel [34].

The reception energy consumption can be calculated as

$$E_{rece}(i) = p_r \cdot \frac{b_{rece}(i)}{u_r}, \tag{6}$$

where p_r and u_r denote the node receiving power and rate, respectively. The total received data size is

$$b_{rece}(i) = \sum_{v_k \in V, v_k \neq v_i} x_{k,i} \cdot b_{data}(k), \tag{7}$$

where $b_{data}(k)$ is the packet generated by v_k, and $x_{k,i}$ is a binary variable. When node v_k successfully transmits data to node v_i, $x_{k,i} = 1$; otherwise, $x_{k,i} = 0$.

3.4 Data collection delay model

Dynamic clustering generates time-varying CH sets $Q = \{q_1, q_2, \ldots, q_M\}$. The set of nodes within the m^{th} cluster is C_m. A stable communication link is established when AUV enters the communication range of the CH node.

The base station on water surface is recorded as virtual CH q_0. AUV cruise path L_{auv} departs from q_0, traverses all CHs in sequence, and returns to q_0, as shown in Fig.3. Ignoring data transmission time, data collection delay is determined by AUV travel path and speed:

$$L_d = \frac{L_{auv}}{v_{auv}}. \tag{8}$$

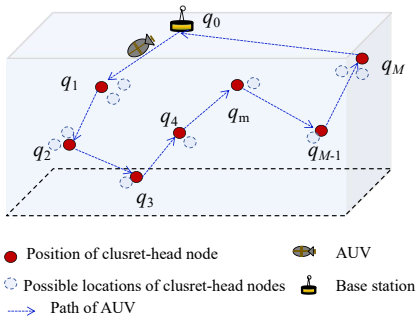


Fig. 3: A mobility path of AUV

3.5 Problem statement

The purpose of this work is to minimize the data collection delay under dynamically changing network topologies. Based on the above analysis, the objective function and constraint conditions are formulated as follows:

$$\min \sum_{i=1}^{M+1} \sum_{j=1}^{M+1} \frac{d(q_i(t_{0,i}), q_j(t_{i,j}))}{v_{auv}} \cdot a_{ij}$$

$$s.t. \sum_{q_i \in Q} a_{ij} = 1, \quad \forall j \in \{1, 2, \ldots, M+1\}, i \neq j \tag{9}$$

$$\sum_{q_j \in Q} a_{ij} = 1, \quad \forall i \in \{1, 2, \ldots, M\}, i \neq j \tag{10}$$

$$\sum_{i=1}^{M+1} \sum_{j=1}^{M+1} a_{ij} = M + 1 \tag{11}$$

$$a_{ij} \in \{0, 1\}, \quad \forall i, j \in \{1, 2, \ldots, M, M+1\} \tag{12}$$

where $t_{0,i}$ represents the AUV travel time from the base station to CH q_i, and a_{ij} is a binary variable indicating AUV cruising route, where $a_{ij} = 1$ for movement from q_i to q_j and $a_{ij} = 0$ otherwise. The problem belongs to high-complexity dynamic TSP due to time-varying CH positions, which is solved by the proposed DCADNT algorithm in Section IV.

4 DCADNT algorithm design

The proposed DCADNT algorithm consists of three interdependent phases: dynamic clustering with multi-criteria CH selection, propagation delay-aware adaptive dynamic transmission, and mobility prediction-based reliable AUV data collection, as shown in Fig.4.

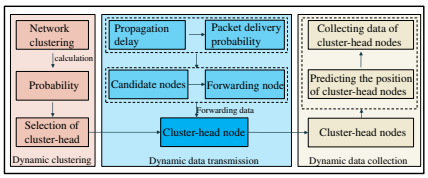


Fig. 4: The process of DCADNT

4.1 Dynamic clustering

Node mobility trajectories are simulated via the mobility model in Formula (3). Network topology perception and dynamic clustering are implemented through bidirectional information interaction. The base station broadcasts beacon packets to

implement network topology perception. Nodes forward beacons to neighbors, and communication connected nodes form independent clusters[35] [36]. The total cluster quantity M and intra-cluster node set C_m $(m = (1, 2, \cdots, M))$ are determined accordingly.

CH selection comprehensively considers three indicators: node closeness centrality, residual energy and data load. Closeness centrality quantifies the average shortest path proximity to intra-cluster nodes:

$$C_{cn}(i) = \frac{n_m - 1}{\sum\limits_{v_k \in C_m, k \neq i} e_{num}(i,k)}, \tag{13}$$

where n_m is the number of nodes in the m^{th} cluster, and $e_{num}(i,k)$ is the number of edges in shortest path between node v_i and v_k, $v_k \in C_m$ [37].

The probability that any node v_i in a cluster is selected as CH node at time t can be calculated by (14).

$$P_{CH}(i,t) = \left(\gamma \cdot \frac{E_{res}(i,t)}{E_0} + (1-\gamma) C_{cn}(i)\right) \frac{b_{tran}(i,t)}{\max\limits_{v_i \in V}(b_{tran}(i,t))}, \tag{14}$$

The node with maximum P_{CH} will be selected as CH. Node mobility induces dynamic network clustering, necessitating continuous re-selection of CH to maintain optimal network performance.

4.2 Propagation delay-aware dynamic transmission

Limited acoustic propagation speed causes non-negligible transmission delay. The end-to-end propagation delay between v_i and v_j is formulated as

$$D_c(i,j,t) = \frac{b_{tran}(i,t)}{c_b} + \frac{d(v_i, v_j, t)}{v_{uw}}, \tag{15}$$

where c_b is channel capacity, v_{uw} is transmission speed of underwater acoustic communication.

The packet delivery probability with a length of b-bit based on propagation delay is defined as [9]

$$P_c(i,j,t) = \left(1 - p_e(i,j,t)\right)^b, \tag{16}$$

where $p_e(i,j,t)$ is the bit error rate with distance $d(v_i, v_j, t)$, which can be calculated by formula (17)

$$p_e(i,j,t) = \frac{1}{2} \cdot \left(1 - \sqrt{\frac{\Gamma(i,j,t)}{1 + \Gamma(i,j,t)}}\right), \tag{17}$$

where $\Gamma(i,j,t)$ is the average signal-to-noise ratio (SNR) for the link from v_i to v_j. Given transmission power p_t and communication frequency f_c, the SNR is formulated as:

$$\Gamma(i,j,t) = \frac{p_t}{A(d(v_i, v_j, t) N(f_c) B_w}, \tag{18}$$

where B_w indicates noise bandwidth, $N(f_c)$ is the underwater noise.

To ensure reliable communication, link availability and packet delivery probability must exceed predefined thresholds throughout the entire transmission duration. This work discretizes total transmission delay $(D_c(i,j,t))$ into multiple equal-length time

slots and predicts node coordinates in each slot based on historical mobility information. Nodes that maintain both ($P_c(i,j,t+\Delta t) \geq p_0$) and valid communication distance during the whole period are selected as candidate forwarding nodes, formulated as:

$$\begin{aligned} f_i^{cw}(t) = \{v_j | P_c(i,j,t+\Delta t) \geq p_0 \\ \& \quad d(v_i, v_j, t) \leq R_c\}. \end{aligned} \tag{19}$$

All qualified neighbors form the candidate forwarding node set $F_i^{cw}(t)$. For data forwarding, the optimal next-hop node is selected from $F_i^{cw}(t)$ by jointly considering residual energy and proximity to CHs. The probability of node v_k selection as a forwarding node of v_i at time t can be expressed as

$$P_{f_i^{cw}}(k,t) = \lambda_1 \cdot \frac{E_{res}(k,t)}{E_0} + (1-\lambda_1) \cdot \max \mathbf{D}_{\mathbf{col}}^{Q}(k,i,t), \tag{20}$$

where weighting factor $0 < \lambda_1 < 1$. Term $\mathbf{D}_{\mathbf{col}}^{Q}(k,i,t)$ quantifies the advantage of candidate node v_k being closer to CHs compared with source node v_i:

$$\mathbf{D}_{\mathbf{col}}^{Q}(k,i,t) = \frac{\mathbf{d}_{\mathbf{col}}^{Q}(i,t) - \mathbf{d}_{\mathbf{col}}^{Q}(k,t)}{\max \mathbf{d}_{\mathbf{col}}^{Q}(i,t)} \tag{21}$$

$\mathbf{d}_{\mathbf{col}}^{Q}(i,t) = (d(v_i,q_1,t), \ldots, d(v_i,q_j,t), \ldots, d(v_i,q_M,t))^T$ represents the distance vector from v_i to CH nodes Q at time t, $\mathbf{d}_{\mathbf{col}}^{Q}(k,t)$ is the corresponding distance vector of candidate node v_k.

If node v_k is selected as the forwarding node at time t, its residual energy needs to meet (22).

$$\begin{aligned} E_{res}(k,t) \geq p_t \cdot A(R_c, f) \cdot \frac{b_{tran}(i,t)}{u_t} + \\ p_t \cdot A(R_c, f) \cdot \frac{b_{tran}(k,t)}{u_t} + p_r \cdot \frac{b_{tran}(i,t)}{u_r}. \end{aligned} \tag{22}$$

Under the condition that residual energy satisfies (22), the node with the maximum $P_{f_i^{cw}}(k,t)$ is selected as the forwarding node. The complete propagation delay-aware dynamic transmission logic is summarized in Algorithm 1.

4.3 Mobility prediction-based AUV data collection

AUV periodically executes adaptive data collection targeting dynamically updated CHs. It first broadcasts beacon packets to all CH nodes to acquire their coordinates and data information. Combined with the layered mobility model, AUV predicts CH drift trajectories and future positions. According to the minimum-delay TSP optimization objective, AUV dynamically plans cruising paths and sequentially collects data from predicted CH positions. AUV updates CH information and re-optimizes trajectories after each collection, as illustrated in Fig. 5. The detailed procedure is presented in Algorithm 2.

5 Performance Evaluation

This section evaluates the performance of the proposed DCADNT algorithm under varying parameter settings. Comparative simulations are conducted against three baseline algorithms: DDCA [18], ACRL[29], and HAMA [30]. For DDCA, AUV optimizes

Algorithm 1 The propagation delay-aware dynamic transmission algorithm

Require: V, n, R_c, Q , t, p_0, u_t, u_r, p_t, p_r, E_0, λ_1, c_b, v_{uw}
Ensure: The forwarding node

for $\forall v_i \in V$ **do**
  Initialize the candidate forwarding node set $F_i^{cw}(t)$ of v_i
  for j=1 to n **do**
    if $d(v_i, v_j, t) \leq R_c$ & $E_{res}(j,t) > 0$ **then**
      $D_c(i,j,t) = \dfrac{b_{tran}(i,t)}{c_b} + \dfrac{d(v_i,v_j,t)}{v_{uw}}$
      for t_1=0 to $\lceil D_c(i,j,t) \rceil$ **do**
        Calculate the packet delivery probability $P_c(i,j,t+t_1)$
      end for
    end if
    if $\min\limits_{0 \leq t_1 \leq \lceil D_c(i,j) \rceil} (P_c(i,j,t+t_1)) \geq p_0$ **then**
      $F_i^{cw}(t) \leftarrow F_i^{cw}(t) \cup \{v_j\}$
    end if
  end for
  for $\forall v_k \in F_i^{cw}(t)$ **do**
    if $E_{res}(k,t) \geq p_t \cdot A(R_c, f) \cdot \dfrac{b_{tran}(i,t)}{u_t} + p_t \cdot A(R_c, f) \cdot \dfrac{b_{tran}(k,t)}{u_t} + p_r \cdot \dfrac{b_{tran}(i,t)}{u_r}$ **then**
      $\mathbf{d}^Q_{\mathbf{col}}(i,t) = (d(v_i,q_1,t) \ldots d(v_i,q_j,t) \ldots d(v_i,q_M,t))^T$
      $\mathbf{d}^Q_{\mathbf{col}}(k,t) = (d(v_k,q_1,t) \ldots d(v_k,q_j,t) \ldots d(v_k,q_M,t))^T$
      $\mathbf{D}^Q_{\mathbf{col}}(k,i,t) = (\mathbf{d}^Q_{\mathbf{col}}(i,t) - \mathbf{d}^Q_{\mathbf{col}}(k,t)) / \max \mathbf{d}^Q_{\mathbf{col}}(i,t)$
      $P_{f_i^{cw}}(k,t) = \lambda_1 \cdot \dfrac{E_{res}(k,t)}{E_0} + (1-\lambda_1) \cdot \max \mathbf{D}^Q_{\mathbf{col}}(k,i,t)$
    end if
  end for
  $f_i^{cw}(t) = \arg \max\limits_{v_k \in F_i^{cw}(t)} P_{f_i^{cw}}(k,t)$
end for

cruising paths based on predicted node positions to reduce travel distance. ACRL adopts FCM and FA to optimize clustering and CH selection, combined with Q-learning for AUV path planning. In HAMA, AUV follows a fixed spiral trajectory, while ordinary nodes forward data to relay nodes near the predefined route.

5.1 Simulation Scenarios and Parameter Settings

Simulations are implemented in a 3D underwater network with a size of $|10^3 * 10^3 * 500m^3|$. The surface base station and initial AUV position are both set to (500, 500, 0). Node mobility is governed by layered ocean current characteristics. The whole water body is divided into $\mathfrak{h}$=5 horizontal layers. The weighting coefficients are set to γ=0.6 (CH selection) and λ_1=0.5 (forwarding node selection) throughout the simulations.

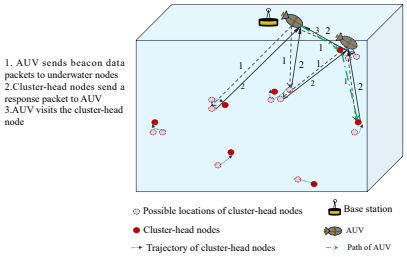


Fig. 5: The process of data collection

Algorithm 2 Mobility prediction-based AUV data collection

Require: V, Q , t_0, q_0
Ensure: The path of AUV $p*$

Initialization path, $p* = [q_0]$
AUV sends beacon data packets to underwater nodes
Nodes storing data are marked as cluster-head nodes
The number of CH nodes is M
Update the set of CH nodes Q
CH nodes send a response packet to AUV
Initialization the position of AUV, $q_{auv} \leftarrow q_0$
while $Q \neq \varnothing$ **do**
    j=1
    while $j \leq M$ **do**
        The trajectory and future position coordinates of cluster-head node q_j are calculated by formula (3)
        Calculate the distance of AUV movement to the predicted node position $d(q_{auv}, q_j)$
        $j = j + 1$
    end while
    $q_k = \arg\min_{q_j \in Q} d(q_{auv}, q_j)$
    $p* \leftarrow p* \cup \{q_k\}$
    $Q \leftarrow Q - \{q_k\}$
    $M = M - 1$
end while

The simulation parameters and system inertial parameters ξ are listed in Table 1 and Table 2. The aforementioned models and parameters are extensively employed in UWSN simulations. All simulation results are averaged over 100 independent repeated experiments to guarantee statistical validity.

5.2 Performance evaluation

1) Data collection delay: Fig.6 compares the data collection delay of all schemes with varying node numbers under fixed conditions of R_c=200m and v_{auv}=5m/s.

Table 1: The basic simulation parameters

Relevant parameter	Value	Relevant parameter	Value
n	50-80	R_c	200m
λ	1.5	E_{elec}	5 $\times 10^{-4}$ J/bit
E_0	5000J	b_{data}	5kbit
p_t	2W	p_r	0.5W
u_t	3kbps	u_r	8kbps

Table 2: The relevant parameters for inertial parameter ξ

Parameter	Value	Parameter	Value
A_R	0.16m^2	ρ	1.03g/cm^3
$\mathbb{V}$	0.025m^3	σ	0.23

The collection delay of DDCA, ACRL, and DCADNT increases as node density grows. DDCA yields the highest delay due to its full-node traversal mechanism, which introduces substantial AUV cruising overhead. ACRL achieves a lower delay than DCADNT by merely collecting CH data while neglecting isolated mobile nodes. HAMA maintains a constant delay owing to its fixed periodic AUV cruising strategy. At $n = 100$, the proposed DCADNT reduces data collection delay by 34.1% and 21.7% compared with DDCA and HAMA, respectively.

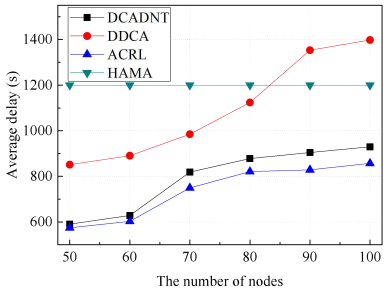


Fig. 6: Data collection delay

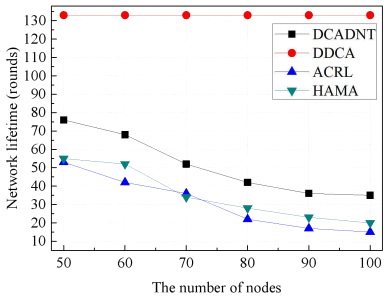


Fig. 7: Comparison of lifetime with different number of nodes

2) Network lifetime: Fig.7 illustrates the network lifetime variation with node quantity. Overall network lifetime declines as sensor density grows. Dense deployment increases data aggregation load on CHs, which accelerates network energy consumption. Unlike ACRL, DCADNT supports data collection from both CHs and isolated nodes, generating more reasonable dynamic cluster partitions. Although DCADNT

sacrifices partial delay performance, it effectively prolongs network lifetime compared with ACRL. For DDCA, AUV collects data from all nodes in each round, resulting in stable per-round energy consumption. Accordingly, its network lifetime is insensitive to node density and only depends on initial node energy and packet size.

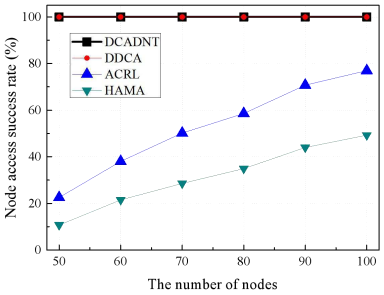


Fig. 8: Comparison of success rate of node access

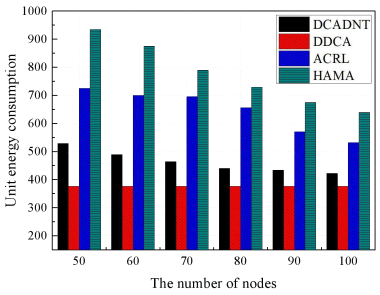


Fig. 9: Comparison of unit energy consumption

3) Node access success rate: Fig.8 characterizes the node access success rate of all algorithms under different node densities. DDCA achieves 100% access success rate by collecting data from all sensors one by one. Similarly, DCADNT maintains full acquisition success rate by adaptively accessing dynamic CH nodes, isolated nodes, and sub-network nodes under time-varying topologies. In contrast, ACRL merely retrieves CHs data and abandons isolated nodes. Combined with mobility and propagation delay induced forwarding failures, its access success rate cannot reach 100% (though it gradually rises with denser sensors providing more relay opportunities). HAMA achieves the lowest success rate of node access, since node mobility and time-varying propagation delay cause incomplete data forwarding, while fixed AUV cruise trajectories frequently fail to capture mobile data nodes.

4) Unit energy consumption: Fig.9 presents the unit energy consumption of all schemes versus node density. Unit energy consumption for packet collection gradually declines with increased node quantity. DDCA exhibits stable unit energy consumption, as its sequential single-node collection mode produces fixed energy overhead for identical packet scales. Benefiting from the superior success rate of node access performance, DCADNT achieves lower unit energy consumption and higher energy efficiency compared with ACRL.

5) Influence of communication radius: Fig.10 analyzes latency variation with different communication radii under n=50 and v_{auv}=5m/s. For both ACRL and DCADNT, enlarged communication radius reduces collection delay by expanding cluster coverage and optimizing AUV cruising paths. Under small radius ($R_c = 150m$), DCADNT generates more dynamic clusters and isolated nodes than fixed-cluster ACRL, resulting in slightly higher delay. As R_c increases, cluster quantity drops sharply and significantly cuts AUV sailing overhead of DCADNT. When $R_c = 400m$,

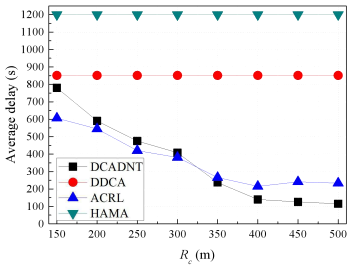


Fig. 10: Comparison of collection delay with R_c

all nodes merge into one single cluster, and DCADNT only needs to visit one cluster head, thereby achieving a lower delay. Further expanding the R_c brings negligible delay variation, and DCADNT still maintains superior performance.

6) The impact of water flow: Water flow velocity determines the mobility intensity of underwater sensor nodes, where faster currents induce more drastic node movement. Fig.11 and Fig.12 analyze the joint effects of AUV velocity, water flow velocity, and communication radius on collection delay. HAMA is excluded from this analysis due to its fixed cruising cycle and invariant delay. Fig. 11 indicates that low current flow velocity causes slight node movement, and increasing AUV speed effectively reduces collection delay. Once AUV speed exceeds a critical threshold, the delay of DCADNT approximates that of ACRL. At low AUV sailing speed, even mild node movement greatly increases the collection latency. DDCA always achieves the worst delay performance since it requires sequential full-node access.

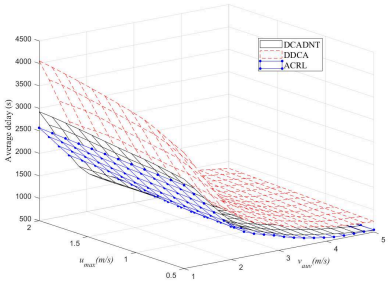


Fig. 11: The impact of u_{max} and v_{auv}

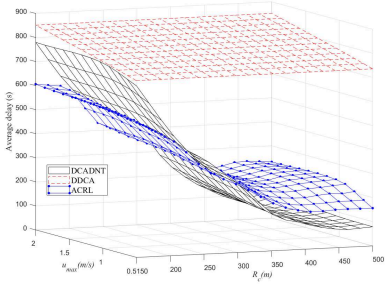


Fig. 12: The impact of u_{max} and R_c

Fig.12 further illustrates the coupling effect of communication radius and maximum flow velocity. Different from DDCA and HAMA, which are insensitive to communication radius, DCADNT and ACRL exhibit obvious performance differences under varying parameter combinations. With fixed flow velocity, expanding communication radius reduces the number of dynamic clusters and CH nodes in DCADNT, and gradually outperforming the fixed-cluster ACRL in delay. With fixed communication radius, increased flow velocity aggravates node mobility and raises the collection delay.

Overall, the proposed DCADNT algorithm demonstrates strong adaptability to dynamic UWSN environments. It guarantees complete node access success rate via propagation delay-based link reliability evaluation, extends network lifetime compared with ACRL, and drastically reduces collection delay relative to DDCA.

6 Results and Discussion

Aiming at network topology variations caused by underwater sensor drift, this paper proposes DCADNT, a dynamic topology-oriented AUV data collection algorithm for UWSN systems. The framework implements dynamic network partitioning and adaptive CHs selection for drifting sensors; by calculating propagation delay dependent packet delivery probability, DCADNT optimizes network energy depletion and data collection delay simultaneously. The performance of DCADNT is compared with that of other data collection strategies. Though DCADNT exhibits slightly higher collection delay than ACRL, it achieves remarkable improvements in network lifetime, node access success rate and unit data energy efficiency. Compared with DDCA, DCADNT matches its full node access success rate while significantly cutting AUV collection delay delivering superior overall comprehensive performance.

However, in the process of data collection, the influence of the current model on the trajectories of AUVs is not considered, and this will be the focus of our future work. In mobile UWSN scenarios, planning a smooth AUV path that can eliminate the adverse effects of water flow is also a key research direction that needs to be focused on in future underwater data collection.

Declarations

- Funding
  This research was supported in part by the Natural Science Foundation of Hebei Province of China (F2026201011), the Natural Science Foundation of Hebei Education Department of China(QN2026833), Beijing-Tianjin-Hebei basic research cooperation project (F2024201070), the Principal's Research Fund of Hebei University (XZJJ202304), scientific research fund of Hebei University (521100224212), and the Tianjin Natural Science Foundation (Grant No. 25JCQNJC00600).
- The authors declare that they have no competing interests.
- Ethics approval and consent to participate
  Not applicable
- Consent for publication
  Not applicable
- Data availability
  The data used to support the results of this study can be obtained from the corresponding author upon request.
- Materials availability
  Materials supporting the results of this study can be obtained upon request from the corresponding author.
- Code availability

The Code used to support the results of this study can be obtained from the corresponding author upon request.

- Author contribution
  Xiaoyun Guang, Chunfeng Liu, Zijuan Liu, Jiaqi Shen, Wenlong He,Yanni Ma, Zhao Zhao designed the study and helped to draft the manuscript. Xiaoyun Guang and Chunfeng Liu wrote the main manuscript text and Zijuan Liu prepared algorithm 1-2, Jiaqi Shen and Wenlong He performed the simulations, and Zhao Zhao prepared figures 1-4, and Yanni Ma checked the format of the entire text. All authors reviewed the manuscript. All authors read and approved the final manuscript.

References

[1] X. Tang, H. Zhang, R. Zhang, D. Zhou, Y. Zhang, and Z. Han, "Robusnt trajectory and offloading for energy-efficient UAV edge computing in industrial internet of things," IEEE Transactios on Industrial Informatics, vol. 20, no. 1, pp: 38-49, 2024.

[2] T. Qiu, Z. Zhao, T. Zhang, C. Chen, and C.L.Philip Chen, "Underwater internet of things in smart ocean: system architecture and open issues," IEEE Transactions on Industrial Informatics, vol. 16, no. 7, pp:4297-4307, 2020.

[3] F. Xing, Y. Tan, Z. Wang, Y. Yue, and H. Yin, "Joint power allocation for multiple nodes in serial relaying networks over underwater wireless optical channels," Computer Networks, vol. 257, pp: 110941, 2025.

[4] C. Li, X. Du, L. Wang, X. Tian, and Z. Wang, "Reliable energy-efficient routing protocol based on anomalous detection and AUV-aid for underwater sensor networks," Journal on Communications, vol. 46, no. 1, pp: 205-212, 2025.

[5] T. Zhang, Y. Gou, J. Liu and J. -H. Cui, "Traffic load-aware resource management strategy for underwater wireless sensor networks," IEEE Transactions on Mobile Computing, vol. 24, no. 1, pp: 243-260, 2025.

[6] M. Chaudhary, N. Goyal, A. Benslimane, L. K. Awasthi, A. Alwadain, and A. Singh, "Underwater wireless sensor networks: enabling technologies for node deployment and data collection challenges," IEEE Internet of Things Journal, vol. 10, no. 4, pp: 3500-3524, 2023.

[7] S. Z. Feng and F. Q. Li, "An introduction to marine science," Beijing, China: Higher Education Press, 1999, pp: 164-167.

[8] A. Ye and F. Li, "Physical oceanography," Qingdao, China: Ocean University Press, 1992, pp. 252-262.

[9] G. Han, S. Shen, H. Song, T. Yang and W. Zhang, "A stratification-based data collection scheme in underwater acoustic sensor networks," IEEE Transactions on Vehicular Technology, vol. 67, no. 11, pp: 10671-10682, Nov. 2018.doi: 10.1109/TVT.2018.2867021.

[10] J. Li, "A survey of routing algorithms for underwater wireless sensor networks," Journal of Computing and Electronic Information Management, vol. 16, no. 1, pp:60-62, 2025.

[11] D. Halkin, and T. Rossby, "The structure and transport of the gulf stream at 73w," Journal of Physical Oceanography, vol. 15, no. 11, pp: 1439-1452, 2010.

[12] M. Akyildiz, "Three-dimensional and two-dimensional deployment analysis for underwater acoustic sensor networks," Ad Hoc Networks, 2009.

[13] K. Ji, C.Lin, J. Ren, Q. Wang, X. Fan, and Z. Luo, "Underwater data collection scheme based on LLMs," IEEE INFOCOM 2026 - IEEE Conference on Computer Communications, pp:1-10, 2026.

[14] N. Suriya, and M. Palanivelan, "Archimedes chicken swarm optimization?based routing for internet of underwater wireless sensor networks," International Journal of Communication Systems, vol. 38, no. 5, pp: 6052.1-6052.20, 2025. DOI:10.1002/dac.6052.

[15] X. Zhuo, M. Liu, Y. Wei, G. Yu, and R. Sun, "AUV-aided energy-efficient data collection in underwater acoustic sensor networks," IEEE Internet of Things Journal, vol. 7, no. 10, pp: 10010-10022, 2020.

[16] Y. Chen, R. Zhu , A. Boukerche, and Q. Yang, "AUV-assisted data collection using hybrid clustering and reinforcement learning in underwater acoustic sensor network," Ad Hoc Networks, vol. 178, 2025.

[17] X. Zhuo, W. Wu, L. Tang, F. Qu, and X Shen, "Value of information-based packet scheduling scheme for AUV-assisted UASNs," IEEE Transactions on Wireless Communications, vol. 23, no. 7, pp: 7172-7185, 2024.

[18] X. Guang, W. Qu, C. Liu, and T. Qiu, "DDCA: A dynamic data collection algorithm in mobile underwater wireless sensor networks," IEEE 24th International Conference on Computer Supported Cooperative Work in De-sign (CSCWD), pp: 819-824, 2021.

[19] J. Li, and Q. Chen, "A multi-AUV adaptive collaborative target coverage algorithm for unknown environment," Ad Hoc Networks, vol. 180, pp: 104033, 2026.

[20] L. Liu, R. Wang, and F. Xiao, "Topology control algorithm for underwater wireless sensor networks using GPS-free mobile sensor nodes," Journal of Network

and Computer Applications, vol. 35, no. 6, pp: 1953-1963, 2012.

[21] L. Liu, N. Zhang, and Y. Liu, "Topology control models and solutions for signal irregularity in mobile underwater wireless sensor networks," Journal of Network and Computer Applications, vol. 51, pp: 68-90, 2015.

[22] L. Liu, and Y. Liu, "On exploring data forwarding problem in opportunistic underwater sensor network using mobility-irregular vehicles," IEEE Transactions on Vehicular Technology, vol. 64, no. 10, pp: 4712-4727, 2015.

[23] L. Liu, R. Wang, and J. Wu, "On the adaptive data forwarding in opportunistic underwater sensor networks using GPS-free mobile modes," Journal of Parallel and Distributed Computing, vol. 122, pp: 131-144, 2018.

[24] L. Liu, W. Ran, D. Guo, and X. Fan, "Message dissemination for throughput optimization in storage-limited opportunistic underwater sensor networks," 2016 13th Annual IEEE International Conference on Sensing, Communication, and Networking (SECON), 2016.

[25] L. Liu, R. Wang, G. Xiao, and D. Guo, "On the throughput optimization for message dissemination in opportunistic underwater sensor networks," Computer Networks, vol. 169, pp: :107097, 2020.

[26] W. Khan, H. Wang, M. S. Anwar, M. Ayaz, S. Ahmad, and I. Ullah, "A multi-layer cluster based energy efficient routing scheme for UWSNs," IEEE Access, 2019.

[27] N. Jiang, Q. Zhao, and J. Wang, "Deep reinforcement learning-based path planning method for underwater gliders in unknown 3D marine environment," Ships and Offshore Structures, vol. 20, no. 1, pp: 121-132, 2025.

[28] X. Cao, H. Sun and L. Guo, "Potential field hierarchical reinforcement learning approach for target search by multi-AUV in 3D underwater environments," International Journal of Control, vol. 93, no. 7, pp: 1677-1683, 2020.

[29] Y. Chen, R. Zhu, A. Boukerche, and Q. Yang, "AUV-assisted data collection using hybrid clustering and reinforcement learning in underwater acoustic sensor networks," Ad Hoc Networks, vol. 178, pp: 103877, 2025.

[30] G. Han, X. Long, C. Zhu, M. Guizani and W. Zhang, "A high-availability data collection scheme based on multi-AUVs for underwater sensor networks," IEEE Transactions on Mobile Computing, vol. 19, no. 5, pp. 1010-1022, 1 May 2020.

[31] M. Al-Bzoor, E. Al-Assem, L. Alawneh, and Y. Jararweh, "Autonomous underwater vehicles support for enhanced performance in the internet of underwater things," Transactions on Emerging Telecommunications Technologies, vol. 32, no. 3, pp: 1-19, 2021.

[32] X. Hou, J. Wang, T. Bai, Y. Deng, Y. Ren, and L. Hanzo, "Environment-aware AUV trajectory design and resource management for multi-tier underwater computing," IEEE Journal on Selected Areas in Communications, vol. 41, no. 2, pp: 474-490, 2023.

[33] Z. Fang, J. Wang, J. Du, X. Hou, Y. Ren, and Z. Han, "Stochastic optimization-aided energy-efficient information collection in internet of underwater things networks," IEEE Internet of Things Journal, vol. 9, no. 3, pp: 1775-1789, 2022.

[34] M. Huang, K. Zhang, Z. Zeng, T. Wang, and Y. Liu, "An AUV-assisted data gathering scheme based on clustering and matrix completion for smart ocean," IEEE Internet of Things Journal, vol. 7, no. 10, pp: 9904-9918, 2020.

[35] R. Diamant, P. Casari, F. Campagnaro, O. Kebkal, V. Kebkal, and M. Zorzi, "Fair and throughput-optimal routing in multi-modal underwater networks," IEEE Transactions on Wireless Communications, vol. 17, no. 3, pp: 1738-1754, 2018.

[36] A. Camillo', M. Nati, C. Petrioli, M. Rossi, and M. Zorzi, "IRIS: integrated data gathering and interest dissemination system for wireless sensor networks," Ad Hoc Netw., vol. 11, no. 2, pp: 654-671, 2013.

[37] D.L. Hansen, B. Shneiderman, M.A. Smith, and I. Himelboim, "Social network analysis: measuring, mapping, and modeling collections of connections," Analyzing Social Media Networks with NodeXL, 2020.